



# Aircraft Wake Vortex Detection Using Continuous-Wave Radar

*James M. Hanson and Frank J. Marcotte*

**T**he Applied Physics Laboratory designed and constructed a bistatic continuous-wave radar system for experiments in aircraft wake vortex detection. Acoustic pumping was evaluated as a possible technique to enhance overall performance. The radar and acoustic systems were installed at the Baltimore–Washington International Airport in the fall of 1996. Controlled experiments using a NASA C-130 aircraft are discussed, and some preliminary results are presented.

(Keywords: Bistatic radar, Radio-acoustic sounding, Wake vortex.)

## INTRODUCTION

The lifting surfaces of all aircraft produce wake vortices to some extent. The vortex created by a large aircraft such as a 757 can have a catastrophic effect on a small airplane following closely behind. According to the National Transportation Safety Board, wake vortex encounters caused at least 51 incidents in the United States between 1983 and 1993.

Protection against wake vortex turbulence hazards requires that a large distance be maintained behind heavy aircraft during takeoff and landing operations. To ensure safety, spacing is currently determined assuming worst-case vortex conditions. This may take into account the types of aircraft involved but does not consider the presence or absence of atmospheric conditions that also affect vortices. For instance, crosswinds may cause the disturbance to rapidly migrate out of the glide slope (i.e., the prescribed path that an aircraft must follow during an instrument landing).

The Federal Aviation Administration and NASA are working with industry to develop an intelligent system called the Aircraft Vortex Spacing System. This system would determine the optimum aircraft spacing within 2 mi of each runway using a combination of vortex sensors located near the glide slope and a real-time predictive model of the vortex environment. The sensors would be used initially to validate this model. A vortex detection system such as this would not only increase airport productivity by allowing adaptive spacing, but would improve the safety of all aircraft operating around the airport by alerting controllers that hazardous conditions may exist near the runways.

To date, research has focused on the use of active laser or lidar (i.e., laser or light detection and ranging) sensors. These are generally fair-weather sensors, and their performance can be severely degraded by rain or fog. Previous research with Doppler radar has indicated

a potential for this technology to detect strong wind currents even in clear air conditions. In one technique used to perform such detection, acoustic waves are transmitted toward the radar's resolution volume. These waves modulate the atmosphere's refractive index and scatter or reflect the radio waves. Since the acoustic waves are disturbed by the vortex currents, a radar signature should be apparent in the Doppler spectrum. Ultimately, the solution to the vortex sensing problem may be to combine an acoustically pumped radar, a lidar, and direct atmospheric measurements.

In 1996, APL initiated an Independent Research and Development (IR&D) program to investigate the feasibility of using a bistatic continuous-wave radar to detect the presence and severity of strong vortices. Another program objective was to characterize the Doppler signature of a vortex experimentally. Drawing on experience gained developing and testing military radars for many years, APL designed and built such a system comprising a 10-GHz X-band instrumentation radar with independent transmitter and receiver shelters, an acoustic transmitter, and real-time digital signal processors. The Laboratory relied heavily on components already on hand for this effort. The microwave transmitter is based on a 400-W solid-state amplifier developed by the Unisys Corporation and used previously for defense programs. Both the transmitter and receiver employ similar 1.2-m parabolic dish antennas with an approximately 1.6° beamwidth. The acoustic source initially used a horn-loaded 100-W compression driver. However, a 2.4-m parabolic dish and a planar array of speakers have been studied as well.

The system was installed in September 1996 at the Baltimore–Washington International Airport (BWI) for initial testing at the south end of runway 33L; transmitter and receiver shelters were located on opposite sides of the runway. Data were collected using a NASA C-130, which was configured to release environmentally safe smoke to mark its trailing vortices. Processed radar Doppler spectra, raw radar data, and boresight camera video data were displayed in real time and recorded for subsequent analysis. After the BWI tests are completed, we plan to move the system to the John F. Kennedy Airport (JFK) in New York for joint testing with atmospheric sensors supplied by the Department of Transportation Volpe Laboratories as well as lidar systems provided by NASA and the Massachusetts Institute of Technology.

## VORTEX GENERATION AND DESCRIPTION

As mentioned previously, aircraft vortices are generated by the lift-producing surfaces of the aircraft. As the aircraft flies, dominant eddies or vortices develop at the wing tips. This image pair, shown in Fig. 1, is

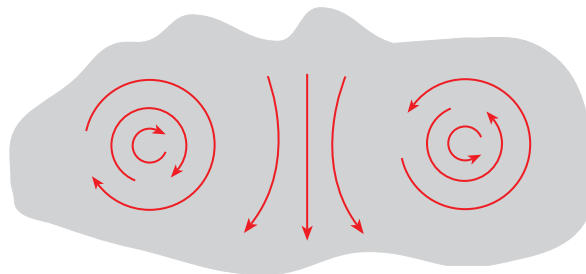


**Figure 1.** Cross-sectional view of a recirculation cell containing the image pair wake vortices. The width of the cell is slightly less than the wing span of the generating aircraft and can contain turbulent velocities up to 60 m/s.

contained in a “recirculation cell.” In benign atmospheric conditions, the recirculation cell slowly descends until ground effects stop the descent or cause the cell to rise. The variability of near-surface conditions (temperature, humidity, wind shear, etc.) can change the drop rate and cause the cell to twist and contort unpredictably.

Generally, the vortex circulation is proportional to  $L/U$ , where  $L$  is the lift generated by the aircraft (equal to the weight in steady flight) and  $U$  is its speed. Core velocities of the vortex can exceed 60 m/s for large aircraft.<sup>1</sup> The core (i.e., cross-sectional diameter at the peak tangential velocity) can be several meters across. The width of the recirculation cell is typically comparable to the aircraft's wing span, well over 40 m for large aircraft.

Knowing the physical makeup of the recirculation cell, the detection system can be tailored accordingly. Lidar systems, with their extremely narrow beamwidths, are ideally suited to detect the peak velocities and the shear within the recirculation cell. Conventional radar, with its much larger search volume, is better suited to detect mean (average) features, such as the Doppler from the overall cell drop rate. A very-high-resolution radar that uses narrow beamwidths, short pulse widths, and low-bandwidth spectral processing, however, could be used as a bridge between conventional radar and lidar systems to detect peak core velocities while retaining the benefits of having a large search volume.

## INSTRUMENTATION RADAR DESIGN ANALYSIS

The weather radar range equation for estimating received power  $P_R$  for a continuous-wave bistatic radar (in which the transmitter and receiver are separated) can be shown to be

$$P_R = \frac{P_T G_T G_R \lambda^2}{(4\pi)^3 R_T^2 R_R^2} \sigma^0 V_C, \quad (1)$$

where

- $P_T$  = the transmitter power,
- $G_T$  and  $G_R$  = the transmitter and receiver antenna gains, respectively,
- $\lambda$  = the wavelength,
- $R_T$  and  $R_R$  = the ranges from the transmitter and receiver to the intersection of the two antenna beams,
- $\sigma^0$  = the target reflectivity per unit volume, and
- $V_C$  = the common volume, which is contained within the intersection of the transmitter's and receiver's conical beams.

For a continuous-wave monostatic radar, the ranges are identical.

From Ref. 2, clear air turbulence reflectivity,  $\sigma^0$ , can be expressed as

$$\sigma^0 = 2\pi k^4 \Phi[2k \sin(\theta_s/2)], \quad (2)$$

where  $k = 2\pi/\lambda$  is the radar wavenumber and  $\theta_s$  is the scattering angle, i.e., the angle at which the radar energy is bent at the common volume from the transmitter toward the receiver and equals  $180^\circ$  for the monostatic case. The spectral representation of the turbulence is given by the characteristic function

$$\Phi(\kappa) = 0.033 C_n^2 \kappa^{-11/3}, \quad (3)$$

where  $\kappa$  is the spatial wavenumber. The value  $C_n^2$  is a structured parameter that is a measure of the intensity of turbulent fluctuations and can range from  $10^{-16} \text{ m}^{-2/3}$  for weak turbulence to  $10^{-12} \text{ m}^{-2/3}$  for very strong turbulence.<sup>2,3</sup>

For a bistatic radar, we approximate the common volume as a rectangular box with width  $R_T \beta_T$ , length  $R_R \beta_R / \sin \theta_s$ , and height equal to the minimum of  $R_T \beta_T$  or  $R_R \beta_R$ , where  $\beta$  is the antenna beamwidth. For a volume equidistant from a transmitter and receiver that are using similar antennas, the volume can be expressed as

$$V_C = \frac{\pi R^3 \beta^3}{4 \sin \theta_s}, \quad (4)$$

where  $\pi/4$  is a shaping factor used to better approximate the rounded features of the volume.

To complete the radar analysis, we must approximate the portion of the common volume that contains the turbulence. The applicable portion of the common

volume depends on the type of vortex feature being detected. For mean vortex features, the applicable volume is the smaller of Eq. 4 or the product of the recirculation cell width, cell height, and the antenna beam width at the common volume ( $R\beta$ ). For detection of peak velocities, the volume is limited to Eq. 4 or the volume of a single vortex, whichever is smaller. For a single vortex, if the core diameter  $D_V$  exceeds  $R\beta$ , we assume that the vortex completely fills the common volume. If, however,  $D_V$  is smaller than  $R\beta$ , the applicable vortex volume  $V_V$  is limited to

$$V_V = \frac{\pi D_V^2 R \beta}{4 \sin \theta_s}. \quad (5)$$

Vortex detection presents several difficult challenges for the radar designer. Most of these problems arise because the vortex itself provides little in the way of a radar target, with the bulk of the return signal coming from refraction of the radar energy as it passes through density differences associated with turbulent fluctuations. Thus, most of the refraction will be away from the radar transmitter (forward scattering), which favors the use of a bistatic radar.

Figure 2 plots reflectivity per unit volume  $\sigma^0$  as a function of scattering angle for strong turbulence ( $C_n^2 = 10^{-12} \text{ m}^{-2/3}$ ). For comparison, a small aircraft will have a reflectivity of approximately 3 dB relative to a  $1\text{-m}^2$  target, often expressed as  $3 \text{ dBm}^2$ . This is 12 orders of magnitude greater than the turbulence reflectivity expected at a modest  $60^\circ$  scattering angle. The reflectivity for the monostatic case ( $\theta_s = 180^\circ$ ) compares favorably with the  $-125 \text{ dBm}^2/\text{m}^3$  value obtained informally from NASA.

Figure 3 provides an estimate of power received from a vortex for several different values of  $C_n^2$ . To generate this figure, the volume was calculated as described previously assuming a core diameter of 9 m. The vortex

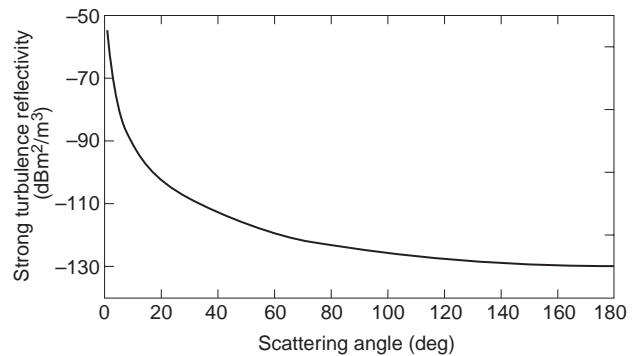
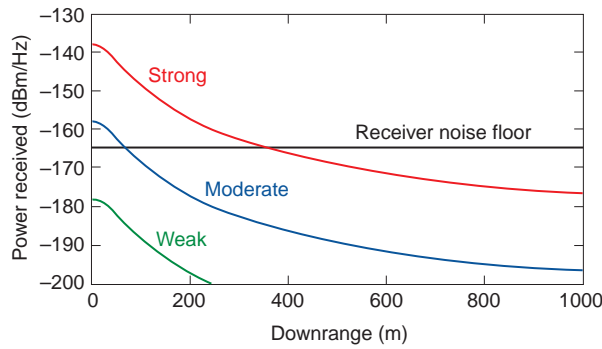


Figure 2. Radar reflectivity of strong clear air turbulence as a function of scattering angle ( $C_n^2 = 10^{-12} \text{ m}^{-2/3}$ ).



**Figure 3.** Estimated power received for various levels of clear air turbulence for a notional APL instrumentation radar. Turbulent fluctuations,  $C_n^2$ , were  $10^{-12}$ ,  $10^{-14}$ , and  $10^{-16} \text{ m}^{-2/3}$  for strong, moderate, and weak turbulence, respectively. Radar specifications are transmitter power = 400 W, beamwidth =  $1.6^\circ$ , transmitter/receiver separation = 1000 m, and vortex height  $\approx 61 \text{ m}$ ; these values are representative of an instrumentation radar that could be developed with existing APL equipment.

was further assumed to contain turbulence traveling up to 15 m/s, spreading the incident energy over  $\pm 150 \text{ Hz}$  of X-band Doppler frequencies to achieve a received power level in dBm/Hz. The receiver noise floor is also indicated in Fig. 3. This figure shows that one can expect to see only moderate to strong turbulence over a limited distance downrange.

The extreme sensitivity required of the radar places severe constraints on the allowable levels of spillover and phase noise. Spillover is the direct transmitter-to-receiver leakage. This signal can enter the receiver through antenna sidelobes or by reflections off ground clutter. A high level of spillover can saturate the receiver, thereby suppressing the target return. It can also impose an unrealistic dynamic range on the system. Phase noise is the noise placed on a signal as it is amplified or similarly processed in an active device. The net effect of phase noise on a signal is to spread energy over adjacent frequencies, possibly obscuring low-level components. Phase noise will exist on all signals in the radar, including the spillover signal, receiver local oscillator signals, and the target signal itself. If acoustic pumping is used, its signal will include some amount of phase noise as well.

For our radar, the greatest threat of phase noise to good performance comes from the spillover signal. Figure 4 shows how the received spectrum may appear. The spectrum contains the vortex signal that is stylized as a noise-like waveform with a finite passband as well as receiver noise and spillover (with its associated phase noise). Pulsed radars can gate out this spillover and phase noise, whereas continuous-wave radars must rely on other means to isolate the transmitter and receiver. Simply increasing transmitter power is not effective, since spillover depends directly on the amount of transmitter power radiated.

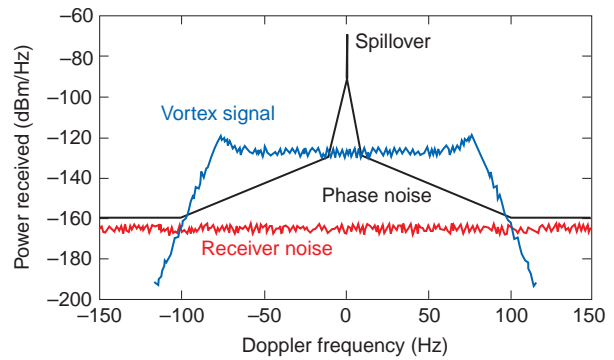


**Figure 4.** Illustration of a received vortex signal spectrum showing the major components. Parameters are the same as in Fig. 3, except for transmitter/receiver separation, which is 1620 m.

For a given vortex height, Fig. 5 presents an estimate of the received signal and spillover power as a function of transmitter/receiver separation. The variation of the spillover level is due to the antenna sidelobes. By judiciously positioning the transmitter and receiver, the effect of spillover can be minimized. Further isolation can be obtained by installing a radar fence between the transmitter and receiver, which also helps minimize spillover due to ground reflections. To achieve an even greater margin, we experimented with an active nuller developed by APL in concert with Raytheon and Watkins-Johnson for the Navy's Tartar program. This device uses an amplified and phase-shifted sample of the transmitter reference to cancel the spillover signal. In our case, the transmitter reference signal was obtained by using a separate receiver channel connected to a horn antenna that was pointed directly from the receiver site to the transmitter.

Figure 5 also indicates that increasing the transmitter/receiver separation provides greater performance for a given vortex height. This occurs because as the distance is increased, the increasing path loss is more than offset by the increasing vortex reflectivity for the shrinking scattering angle. This reasoning breaks down, however, when the scattering angle becomes so small that the

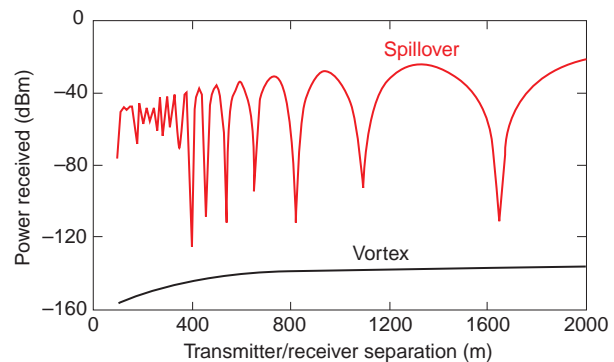


**Figure 5.** Estimated spillover and vortex signal power as a function of transmitter/receiver separation. (Other parameters are the same as those in Fig. 3.)

transmitter and receiver are in each other's main beam, resulting in a huge increase in spillover. A large separation also increases the size of the common volume, making it easier for an aircraft to create a vortex observable by the instrumentation radar, although it also decreases the percentage of the common volume disturbed by the recirculation cell.

## ACOUSTIC PUMPING

The use of a radio acoustic sounding system for atmospheric sensing was proposed as early as 1961 and has been applied by researchers since the late 1970s. The acoustic waves are transmitted toward the common volume and perturb the index of refraction of the air in the volume. If the geometries and frequencies are chosen for Bragg scattering, this refraction disturbance can be observed by the radar. Since wind currents move the Bragg pattern, they can be discerned in the Doppler spectrum of the radar. This technique has been used to measure atmospheric temperature since it affects the local velocity of sound. It can be shown that for Bragg scattering, the optimum acoustic wavelength  $\lambda_a$  is related to the radar wavelength  $\lambda$  and the bistatic scattering angle  $\theta_s$  by the relationship

$$\lambda_a = \frac{\lambda}{2 \sin(\theta_s/2)}. \quad (6)$$

For this X-band radar,  $\lambda$  equals about 0.029 m. Given the geometry of the BWI site, this results in acoustic frequencies ranging from 1.45 to 5.16 kHz, depending on the chosen height for the common volume. Typically, heights from 15 to 50 m have been used.

## THE BWI EXPERIMENT

In March 1996, the NASA Langley Research Center invited APL to take part in a major wake vortex field test being planned for fall 1996 or spring 1997. Officials at BWI were contacted and meetings were held to discuss the possibility of using a site on airport grounds for wake vortex experiments. After studying topographical maps and touring the airport with state officials, suitable locations for the radar transmitter and receiver were found at the south end of runway 33L near Dorsey Road. As evidence of their strong interest in improving airport safety, both the Maryland Aviation Administration and the

Federal Aviation Administration agreed to permit the proposed testing on airport property and have been instrumental in supporting our test efforts at BWI ever since.

Figure 6 shows an aerial view of the BWI test site. The 10-GHz radar transmitter was located on the east side of the runway about 369 m from the centerline of the runway. The receiver (Fig. 7) was situated to the west about 228 m from the centerline. A local contractor performed a survey of the site using a combination of standard optical surveying techniques and a Global Positioning System receiver. These data were required to compute accurate pointing angles for the two radar antennas and to calculate the optimum acoustic frequency based on the geometry.

Each dish antenna was mounted on an electrically steerable pedestal atop a small shelter containing the radar and computer equipment. A 900-MHz digital radio link between computers at the transmitter and receiver sites allowed the two antennas to be steered to any point along the runway glide slope by a single operator at either site. Sensors to measure wind speed and direction were also installed at both sites.

Since testing was to occur near a major highway, wire screen fences were installed at both locations to shield against radar reflections from vehicles. Such reflections can cause a significant problem since the Doppler offset due to trucks passing by is only slightly higher in frequency than that of a wake vortex. The fences served to attenuate the undesirable direct-path spillover signals between the two antennas as described previously. The receiver's radar fence can be seen in Fig. 7.

Initial checkout of the system consisted of antenna alignment testing followed by measurement of receiver



Figure 6. BWI vortex detection test site on runway 33L.



**Figure 7.** Wake vortex receiver site at BWI airport.

signal levels in clear air, both with and without acoustic pumping. In addition, with the runway out of service, the acoustic transmitter was moved to several sites along its centerline, and receiver signal levels were monitored. During this phase of testing, the acoustic transmitter consisted of a Peavy 44T compression driver loaded with a 60° horn. Typically, this was driven with less than 20 W. A digital synthesizer was used to generate a sinusoidal input to the amplifier, which could be varied in frequency.

Testing confirmed that the optimal setup of the acoustic source is to position it vertically and directly in line between the transmitter and receiver along the centerline of the runway. This would place it about 79 m from the south end of the runway. Unfortunately, commercial aircraft are at a very low altitude as they pass over this point, perhaps 15 m or less. At this altitude, ground effects cause the vortex to be unstable and dissipate quickly. To provide a controlled test, arrangements were made for a NASA C-130 aircraft from Wallops Island, Virginia, to fly over the runway on several days. These flights were funded by NASA as a contribution to the APL research efforts.

On 23 September 1996, data were collected at the BWI wake vortex test site using the C-130. This aircraft, a four-engine turboprop transport, was configured to release smoke from its wing tips to mark the trailing wake vortices (see Figs. 8 and 9). Because of mechanical problems, only the left smoke generator on the day of the test. The C-130 made several passes over the runway from the south at varying altitudes, with the majority at about 45 m above the runway. The radar antennas were pointed to place the common volume at 15 or 30 m above the runway and about 9 m to the west. This lateral displacement helped to ensure that the smoke-marked vortex was observed by the radar.

Fortunately, winds were low on the evening of the experiment and the vortex remained fairly stable for



**Figure 8.** A NASA C-130 research aircraft with smoke generator on left wing tip.

several seconds after the aircraft passed the site. A vortex trail can be seen in Fig. 10 from a viewpoint near the end of the runway looking to the south along the glide slope. This photograph was taken several seconds after the passing of the C-130. Since each radar antenna was equipped with a boresight video camera, the transmitter operator was able to tell the receiver operator, via radio, when the vortex trail was within the radar beam. By comparing this announcement to the video from the receiver's boresight camera, we determined when and if the vortex was within the intersection of the two beams.

An audio signal consisting of a continuous tone was transmitted toward the common volume during all of the C-130 passes. With the common volume at 15 m above the runway, the audio frequency was calculated to be 1.45 kHz; at 30 m, a 2.72-kHz signal was used.

Additional C-130 flights were conducted on 29 October and 10 December 1996. Analysis of the data from this testing is still under way, but preliminary results look promising. Figure 11 shows a spectral waterfall plot of one C-130 run. Time is shown on the y axis and relative frequency along the x axis. The prominent peak on the right is the zero Doppler signal centered around the spillover. The smaller peak on the left is applied by the acoustic source. In this figure, the total bandwidth is 10 kHz. The large disturbance at the top corresponds to the point at which the aircraft passed over the common volume. Marks shown on the y axis denote the region where the vortex smoke was visible in both boresight cameras. The vortex turbulence causes a subtle attenuation in the amplitude of the acoustic line, but no Doppler signature is apparent on the acoustic signal for this run.

Figure 12 has been magnified in frequency about the zero Doppler signal to show a 625-Hz band. Clear evidence of the vortex Doppler signature can be seen. This signature was found in several C-130 runs. Further



Figure 9. The C-130 with trailing vortex on approach to BWI.



Figure 10. Smoke-marked vortex as seen several seconds after the C-130 passed by (Fig. 9).

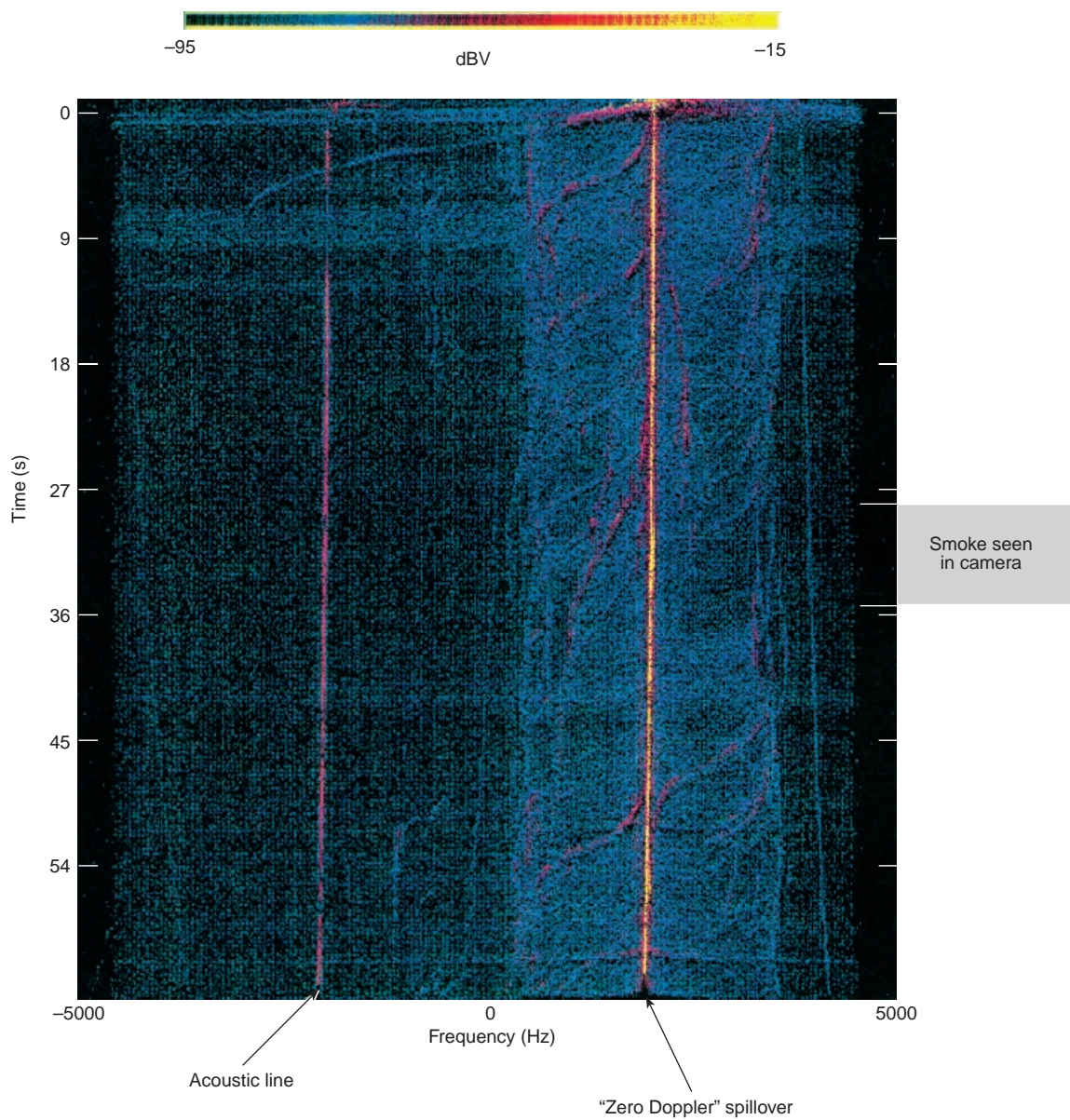
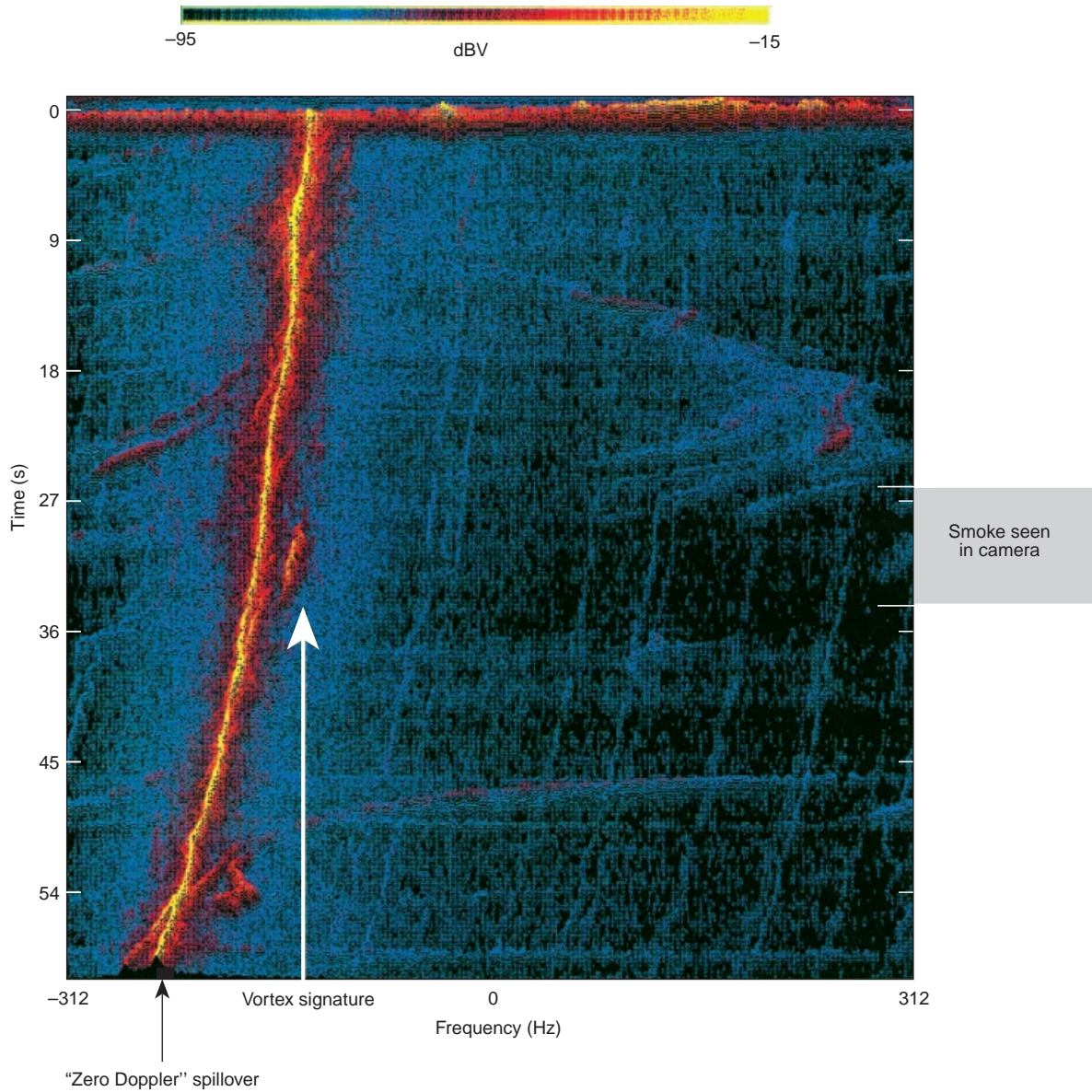


Figure 11. Spectral waterfall of run 9, 29 October 1996, with a 10-kHz bandwidth.



**Figure 12.** Spectral waterfall of run 9, 29 October 1996, with a 625-Hz bandwidth.

analysis, including extensive computer modeling, is being conducted to better characterize these signals.

One area in which the system has evolved is the acoustic transmitter. The driver/horn combination used in September 1996 provided a wide beamwidth (about 60°) to fully illuminate the common volume of the radar. The resulting audio wavefronts were assumed to be planar only over a small portion of the common volume.

A setup using a 2.4-m parabolic reflector was fabricated and installed at BWI for the next phase of testing. This new source provides at least 10 dB more gain in the audio path based on measurements. In addition, a planar array of 16 midrange drivers is being fabricated and will be tested at a future date. Although no current plans exist, the array could be steered by proper phasing between the 16 elements. The additional acoustic gain

from the parabolic reflector allowed the October and December C-130 flight tests to be conducted at a slightly higher altitude, decreasing both spillover leakage and the undesirable reflections from cars.

### THE PROPOSED JFK EXPERIMENT

The Volpe Transportation Systems Center Laboratories and the NASA Langley Research Center are conducting a joint series of wake vortex detection tests at JFK. (The first test was done in November 1996. The second test is scheduled for April 1997; others may be scheduled later in the year.) APL and several other organizations have been invited to participate as well. Although the BWI testing was not completed in time to allow APL participation in the November



experiments, the bistatic radar system may be included in future 1997 tests. Planned wake vortex detection systems to be tested include

- Pulsed coherent lidar system developed by the NASA Langley Research Center
- Continuous-wave lidar system developed by MIT Lincoln Laboratory
- Ground wind line developed by the Volpe Center
- Acoustic-pumped radar experiment developed by APL
- Wake vortex sound detection and ranging system developed by Technology Integration, Inc.
- Wake vortex radar/acoustic sounding system developed by William Rubin

Planned meteorological instrumentation to be tested includes

- Meteorological sound detection and ranging system
- Scintillometer
- Sonic anemometer
- Temperature/relative humidity sensor

The objectives of the JFK test are to compare the performance of these different detection technologies and to correlate meteorological data with the results from the vortex detection sensors. Experiments are planned using commercial aircraft on scheduled take-offs and landings. Additionally, the NASA C-130 with smoke generators may be available for controlled overflights of the site. The proposed site geometry at JFK allows greater separation between the APL transmitter and receiver, and the aircraft will be higher in altitude as they pass over the acoustic transmitter. APL's participation has been welcome; however, continued participation will depend on positive results having been obtained from the BWI tests.

## CONCLUSIONS

A working facility for wake vortex radar experimentation has been established by APL at BWI airport. Many hurdles, both technical and logistical, have been overcome in developing this facility. Although the test results are not yet conclusive, they look promising. A Doppler signature has been found in the data from several, but not all, of the runs. This signature exists to a greater extent on the zero Doppler signal than on the acoustic carrier, implying that the acoustic phenomena seen by other researchers are not fully understood. Data analysis, real-time signal processing, and acoustic transmitter design are all ongoing. The Laboratory is conducting a computer-modeling project in parallel with the hardware experiments. This work draws on experience from submarine wake vortex modeling and will contribute to a better understanding of the physical behavior of the turbulence.

## REFERENCES

- <sup>1</sup> Stewart, E. C., *A Study of the Interaction Between a Wake Vortex and an Encountering Airplane*, AIAA Paper 93-3642, Atmospheric Flight Mechanics Conference, Monterey, CA (Aug 1993).
- <sup>2</sup> Doviak, R., and Zrinc, D., *Doppler Radar and Weather Observations*, 2nd Ed., Academic Press, San Diego, CA (1993).
- <sup>3</sup> *Measurement of Atmospheric Parameters with a Bistatic Radar Supplemented by an Acoustic Source*, Environmental Surveillance Technology Programme, Oslo, Norway (Oct 1995).

ACKNOWLEDGMENTS: The authors are grateful to Dennis Kershner for supporting this work under APL's transportation thrust area. We are also indebted to Robert Neece of the NASA Langley Research Center for providing aircraft services at BWI and technical guidance. The BWI experiment would not have been possible without the diligent efforts of Leo McKenzie in obtaining the necessary approvals and coordinating logistics. In addition, major contributions to the project were made by Allen Bric, Dave Frostbutter, Robert Geller, Hal Gilreath, Alexander Hughes, Russell Iannuzzelli, Bernard Kluga, Larry Manzi, and Terry Schemm.

## THE AUTHORS



JAMES M. HANSON received a B.S. degree in electrical engineering from the Georgia Institute of Technology in 1981 and an M.S. degree in the same field from The Johns Hopkins University in 1986. He joined APL in 1981 and is a member of the Senior Professional Staff in the Air Defense Systems Department's Combat Systems Development Group. Since 1994, he has been the supervisor of the Hardware Design Section of that group. Mr. Hanson has designed data acquisition and signal processing hardware for programs including Standard Missile, Cooperative Engagement Capability, Noncooperative Target Identification, and the U.S./Norway Ocean Radar program. His e-mail address is James.M.Hanson@jhuapl.edu.



FRANK J. MARCOTTE joined APL in 1983 after graduating from Kansas State University with a B.S.E.E. In 1988 he obtained a master's degree in the same discipline from The Johns Hopkins University. Early in his career, Mr. Marcotte was a test and analysis engineer for many Terrier Fire Control System upgrades and used this hardware background to benefit Standard Missile and Aegis programs. He has helped design and develop several coherent instrumentation radars over the years, including radars for antisubmarine warfare and wing-tip vortex detection. Mr. Marcotte is a member of the Air Defense Systems Department's Combat Systems Development Group. His e-mail address is [Frank.Marcotte@jhuapl.edu](mailto:Frank.Marcotte@jhuapl.edu).